Computer solutions of complex biological boundary-value problems
by Reed Allen Parker

A thesis submitted in partial fulfillment of the requirements for the degree of Master of Science in Electrical Engineering
Montana State University
© Copyright by Reed Allen Parker (1984)

Abstract:
The subject of this thesis is to predict the induced spatial current density distribution in biological systems due to a time varying magnetic field. Maxwell's equations are solved using an iterative technique known as the Relaxation Method. Results indicate that the induced spatial currents are a strong function of the particular boundaries of the system being studied. Variations of more than an order of magnitude in a small area are found for some idealized bone fractures. Also the direction of flow tends to be parallel to the bone rather than across the gap as is commonly assumed.

COMPUTER SOLUTIONS OF COMPLEX BIOLOGICAL BOUNDARY-VALUE PROBLEMS

by

Reed Allen Parker

A thesis submitted in partial fulfillment
of the requirements for the degree

of

Master of Science

in

Electrical Engineering

MONTANA STATE UNIVERSITY
Bozeman, Montana

March 1984

MAIN LIB.
N378
P228
cop. 2

APPROVAL

of a thesis submitted by

Reed Allen Parker

This thesis has been read by each member of the thesis committee and has been found to be satisfactory regarding content, English usage, format, citations, bibliographic style, and consistency, and is ready for submission to the College of Graduate Studies.

5/7/84
Date

Bruce R. McLeod
Chairperson, Graduate Committee

Approved for the Major Department

5/7/84
Date

D. A. Pierre
Head, Major Department

Approved for the College of Graduate Studies

5/10/84
Date

Henry L Parsons
Graduate Dean

STATEMENT OF PERMISSION TO USE

In presenting this thesis in partial fulfillment of the requirements for a master's degree at Montana State University, I agree that the Library shall make it available to borrowers under rules of the Library. Brief quotations from this thesis are allowable without special permission, provided that accurate acknowledgment of source is made.

Permission for extensive quotation from or reproduction of this thesis may be granted by my major professor, or in his absence, by the Director of Libraries when, in the opinion of either, the proposed use of the material is for scholarly purposes. Any copying or use of the material in this thesis for financial gain shall not be allowed without my written permission.

Signature Reed A. Parker

Date 7-May-1984

ACKNOWLEDGMENTS

The author would like to thank LaJolla Technology Inc., LaJolla, CA and the Engineering Experiment Station (EES) at Montana State University for funding this work. He is especially grateful to Dr. Bruce McLeod for the suggestions, support, and encouragement during this project. The author is most thankful, however, for the support given to him from his wife and parents.

TABLE OF CONTENTS

	Page
APPROVAL	ii
STATEMENT OF PERMISSION TO USE	iii
VITA	iv
ACKNOWLEDGMENTS	v
TABLE OF CONTENTS	vi
LIST OF FIGURES	viii
ABSTRACT	xi
1. INTRODUCTION	1
2. THE RELAXATION METHOD APPLIED TO ELECTROMAGNETIC FIELDS PROBLEMS	3
Derivation of the Difference equation	3
The Driving Field	4
Implementation of the Relaxation Method in FORTRAN	5
Assumptions	5
3. RESULTS	9
Comparison Between the Two Methods	9
Presentation of Data for the Square Box Example	10
The Bone Models	17
4. CONCLUSIONS	21
REFERENCES CITED	23
APPENDICES	25
APPENDIX A-SQUAREBOX PROGRAM	26
APPENDIX B-ANALYTIC PROGRAM	31
APPENDIX C-DIAGRAMS OF THE BONE MODELS	34

TABLE OF CONTENTS--CONTINUED

Page

APPENDIX D-FLOW AND MAGNITUDE GRAPHS FOR THE BONE BREAK MODELS..... 39

APPENDIX E-TWO DIMENSIONAL GRAPHS OF THE FEMALE-FEMALE BREAK WITH INTERMEDULLARY CANAL..... 54

APPENDIX F-THREE DIMENSIONAL VIEWS OF THE FEMALE-FEMALE BREAK WITH INTERMEDULLARY CANAL..... 59

LIST OF FIGURES

Figure		Page
1.	Coordinate system for the Rectangular Box	9
2.	Magnitude and Flow Graph of Square Box	11
3.	Flow Graph of Square Box	12
4.	Three Dimensional View of Square Box from Edge	13
5.	Three Dimensional View of One Quadrant of the Square Box from Edge	14
6.	Three Dimensional View of Square Box from Inside Corner	14
7.	Three Dimensional View of Square Box from Outside Corner	15
8.	Magnitude of Current Density along Edge of Box	15
9.	Magnitude of Current Density along the Centerline	16
10.	Magnitude of Current Density along the Diagonal	16
11.	Diagram of Female-Female Break with Intermedullary Canal	35
12.	Diagram of Square Break with I.M. Canal (4 mm.)	36
13.	Diagram of Square Break with I.M. Canal (8 mm.)	36
14.	Diagram of Square Break with I.M. Canal (16 mm.)	37
15.	Diagram of Male-Male Break	37
16.	Diagram of Female-Female Break	38
17.	Diagram of Slanted Break	38
18.	Flow Graph of Female-Female Break with I.M. Canal	40
19.	Magnitude and Flow Graph of Female-Female Break with I.M. Canal	41

LIST OF FIGURES--Continued

Page

20. Flow Graph of Square Break (4 mm.)..... 42

21. Magnitude and Flow Graph of Square Break (4 mm.)..... 43

22. Flow Graph of Square Break (8 mm.)..... 44

23. Magnitude and Flow Graph of Square Break (8 mm.)..... 45

24. Flow Graph of Square Break (16 mm.)..... 46

25. Magnitude and Flow Graph of Square Break (16 mm.)..... 47

26. Flow Graph of Male-Male Break..... 48

27. Magnitude and Flow Graph of Male-Male Break..... 49

28. Flow Graph of Female-Female Break..... 50

29. Magnitude and Flow Graph of Female-Female Break..... 51

30. Flow Graph of Slanted Break..... 52

31. Magnitude and Flow Graph of Slanted Break..... 53

32. Graph along Centerline of Break..... 55

33. Graph of Slice Containing Outside Tip..... 56

34. Graph of Slice Containing Center of Bone Face..... 56

35. Graph of Slice Containing Inside Tip..... 57

36. Graph of Outside edge of Bone..... 57

37. Graph of Bone Face from Outside to Inside..... 58

38. Graph of Inside edge of Bone..... 58

39. Three Dimensional View of Break Looking from Outside Towards the Outside Edge of Bone..... 60

40. Three Dimensional View of Break Looking from Outside Towards the Outside Corner of Bone..... 61

LIST OF FIGURES--Continued

Page

41. Three Dimensional View of Break Looking from Center of Break Towards the Bone Face..... 62

42. Three Dimensional View of Break Looking from Center of Break Towards Inside Corner..... 63

43. Three Dimensional View of Break Looking from Inside of I.M. Canal Toward Inside Edge..... 64

44. Three Dimensional View of Break Looking from Inside of I.M. Canal Toward Break..... 65

45. Three Dimensional View of Break Looking from Inside of Bone Toward Break..... 66

46. Three Dimensional View of Break Looking from Outside Towards Break..... 67

ABSTRACT

The subject of this thesis is to predict the induced spatial current density distribution in biological systems due to a time varying magnetic field. Maxwell's equations are solved using an iterative technique known as the Relaxation Method. Results indicate that the induced spatial currents are a strong function of the particular boundaries of the system being studied. Variations of more than an order of magnitude in a small area are found for some idealized bone fractures. Also the direction of flow tends to be parallel to the bone rather than across the gap as is commonly assumed.

CHAPTER 1

INTRODUCTION

The effects of low level electromagnetic energy on biological systems have been documented in several carefully designed experiments [1-4]. This effect can range from increasing the lifespan of mice infected with melanomas (in conjunction with chemotherapy)[1], to modulating the rate of bone fracture healing [2], to adversely affecting the growth of damaged embryos [3]. The exact coupling mechanism between the cell and electromagnetic field is still unknown. In order to determine what this coupling mechanism is, experiments must be designed to have a tight control of variables. Temperature, the process used to test the hypothesis, the system being used, and the electromagnetic fields (both spatially and in the time domain) stimulating the system should be monitored.

Until recently the spatial electric currents induced in biological systems by Helmholz coils were for the most part ignored. McLeod and Sampsel [5,6] have demonstrated that the spatial currents that are introduced into some biological systems can vary by an order of magnitude or more in a very small space. Since the exact coupling mechanism isn't known, researchers should be aware of both the spatial current densities and magnetic fields in their systems.

The work done by McLeod and Sampsel was aimed at simple boundaries whose solution could be determined analytically. In many cases boundar-

ies do not lend themselves to a straightforward analytic solution. The main contribution of this thesis is to present a numerical method to solve some of these complex boundary value problems. Two main systems are looked at separately. A rectangular conducting box is used to verify that the method is accurate, and an idealized two-dimensional bone fracture with different types of bone-flesh boundaries at the site of the fracture is examined in more detail.

Another point that will be addressed in this thesis is how to present the data from these models so that variety of research personnel in such diverse fields as biology, medicine, and engineering can use it. Four methods will be used varying from regular graphs to "three dimensional" views of the system. These methods will be applied to a simple example (a square box) to show how they may be used in conjunction with each other. Finally the bone models will be presented.

CHAPTER 2

THE RELAXATION METHOD APPLIED TO ELECTROMAGNETICS FIELD PROBLEMS

Derivation of the Difference Equation

The differential equation for the $\bar{H}$ field can be derived by starting with Maxwell's fourth equation,

$$\nabla \times \bar{H} = \sigma\bar{E} + \partial(\epsilon\bar{E})/\partial t. \tag{1}$$

Assuming the second term on the right hand side of the equation is small compared to the first term (see discussion on pages 6 and 7 under "assumptions") and taking the curl of both sides yields

$$\nabla(\nabla \cdot \bar{H}) - \nabla^2 \bar{H} = \nabla \times \sigma\bar{E}. \tag{2}$$

The first term on the left hand side is equal to 0 by Maxwell's second equation

$$\nabla \cdot \mu\bar{H} = 0. \tag{3}$$

Substituting Maxwell's third equation,

$$\nabla \times \bar{E} = -\partial(\mu\bar{H})/\partial t, \tag{4}$$

into the right hand side of (2) yields

$$\nabla^2 \bar{H} = \mu\sigma\partial\bar{H}/\partial t. \tag{5}$$

It is seen that this is an equation only in $\bar{H}$. After this equation has been solved the current density $\bar{J}$ can be calculated from (1)

$$\sigma\bar{E} = \bar{J} = \nabla \times \bar{H}. \tag{6}$$

For a two-dimensional case (X-Y plane) with only a Z component of the $\bar{H}$ field, (5) and (6) reduce to

$$\partial^2 H_z/\partial x^2 + \partial^2 H_z/\partial y^2 = \mu\sigma\partial H_z/\partial t, \tag{7}$$

$$J_x = \partial H_z/\partial y, \tag{8}$$

$$J_y = -\partial H_z/\partial x. \tag{9}$$

Equation (7) can be approximated with a difference equation. If we take the continuous function $H_z(x,y)$ and approximate it with a discrete set of points Hx_n,y_n, then the spatial derivatives $\partial^2 H_z/\partial x^2$ can be approximated by the difference equation

$$\partial^2 H_z/\partial x^2 \simeq (Hx_{n+1},y_n + Hx_{n-1},y_n - 2Hx_n,y_n)/\Delta x^2, \tag{10}$$

where Δx is the distance between two consecutive points. If we assume the grid spacing is square ($\Delta x = \Delta y$) with a value of $\Delta 1$ and then substitute the difference approximation into (7), we get the equation for the relaxation method [7],

$$Hx_n,y_n = (Hx_{n-1},y_n + Hx_n,y_{n-1} + Hx_{n+1},y_n + Hx_n,y_{n+1} + 4\Delta 1^2 \mu\sigma\partial Hx_n,y_n)/4. \tag{11}$$

Equations (8) and (9) can be approximated with one of the three point derivative formulas [8],

$$\partial Hx_n,y_n/\partial x \simeq (-3Hx_n,y_n + 4Hx_{n+1},y_n - Hx_{n+2},y_n)/2\Delta 1, \tag{12}$$

$$\partial Hx_n,y_n/\partial x \simeq (-Hx_{n-1},y_n + Hx_{n+1},y_n)/2\Delta 1, \tag{13}$$

$$\partial Hx_n,y_n/\partial x \simeq (Hx_{n-2},y_n - 4Hx_{n-1},y_n + 3Hx_n,y_n)/2\Delta 1. \tag{14}$$

The three point formulas were chosen because their error decreases as a function of $\Delta 1^2$ as opposed to a two-point formula whose error decreases only as a function of $\Delta 1$.

The Driving Field

The driving magnetic field for the iterative solution to the square box was assumed to be uniform to match the assumptions of the analytic method. When the derivative of the magnetic field was calculated for the bone models, the field was not considered uniform. Instead, the equations and program for the magnetic field created by a set of Helmholtz

coils were obtained from Sampsel [6]. The derivative of the magnetic field was then made proportional to the field strength at the point in question. One advantage of using the Helmholtz coils as a driving source, in addition to being more realistic, was that the boundaries perpendicular to the bone could be set in an area of small magnetic field, minimizing their effect of being "artificial boundaries" on the solution.

Implementation of the Relaxation Method in FORTRAN

A representative FORTRAN program that solves the equations for the fields inside a square box is included in Appendix A. The program assumes the driving magnetic field is uniform on the boundaries of the box with its derivative equal to BPRIME. ESTIMATE does the iterating and keeps track of the maximum change between the last two iterations with the variable EPS. When the maximum error criteria is satisfied, the program calculates the current densities at each point with the functions THEL, THER, and THEM. THEL is used to calculate the derivative when the point in question is on the left hand side of the interval, THEM is used to calculate the derivative when the point is in the middle, and THER is used to calculate it when it is on the right hand side. Thus, THEL and THER are used to calculate the current density at a boundary, and THEM is used everywhere else inside the box.

Assumptions

In most simulations there must be some assumptions to simplify the model that is used. In this case seven simplifying assumptions were made. These assumptions are listed and discussed below.

1. It was assumed the system was linear and contained

homogeneous regions.

2. It was assumed that the back emf could be ignored.

3. The conductivity of the fluid pocket and intermedullary canal were assumed to be the same as that of the flesh surrounding the bone.

4. The leg was assumed to be a cylinder with a radius of 32 mm. and a length of 300 mm., the bone was assumed to be a cylinder with a radius of 8 mm., and the intermedullary canal was assumed to be a cylinder with a radius of 4 mm. (when it was included).

5. The width of the break varied from 4 mm. to 16 mm. (i.e. one half to two bone radii).

6. The time-rate-of-change of the magnetic field was assumed to be 3.48 Tesla/second in all cases.

7. The bone was assumed to be a perfect non-conductor.

Assumption (1) was made because biological systems are normally assumed to be linear when dealing with large dimensions. Experiments dealing with low levels and dimensions that are large compared to a single cell show that this is a good approximation. Since this case deals with low frequencies and low drive levels, along with large dimensions, it is a valid assumption. It is probably not valid to make this assumption on a cellular level. At the cellular level there are processes such as active transport of ions across the cell wall, and pockets of protein "floating" in the cell wall which have nonlinear transfer characteristics. These processes make the cell a very nonlinear system.

Assumption (2) was made when the second term of equation (1) was ignored. This assumes the conductivity current term of the equation is much larger than the displacement current term. If we assume a sinusoidal time variation, then the right hand side of (1) becomes $(\sigma + j\omega\epsilon)\bar{E}$. If we assume the point where we must include the second term occurs when $|\sigma| < |10j\omega\epsilon|$, with values of σ for physiological saline (approximately 1 mho/cm) and permittivity (approximately 200), then, the frequency where we have to include the second term occurs at 56 Mhz. Since almost all of the energy in most of the signals being used presently is contained in the frequency region below 1 Mhz., the assumption appears valid in this case.

The next three assumptions were made as a matter of convenience. The conductivities of the three regions may vary slightly, but it will not change the current density pattern enough to justify the extra computer time needed to account for the small variation. The physical dimensions were chosen to be reasonably close to an average leg and bone break, yet allow for easy computer programming. The width of the break was varied to investigate the effect it has on peak current density.

Assumption (6) was made since this is the time-rate-of-change of devices presently in clinical use. If other values are desired then direct scaling can be used. For example, if the time-rate-of-change is doubled, the current density is doubled everywhere.

The last assumption was made to cut down on the time needed to arrive at a solution. The conductivity of the bone is known to be finite, and it is usually assumed to be a tensor quantity. The actual conductivity has been measured, however, and shown to be about two

orders of magnitude smaller than the conductivity of the surrounding flesh. In addition, most of the conductivity is due to saline contained in the canals permeating the bone. The outside of the bone, which is primarily mineral deposits, looks like a non-conducting boundary.

CHAPTER 3

RESULTS

Comparison Between the Two Methods

McLeod [5] has derived the analytic solution for the current density in a rectangular conducting box with a uniform magnetic field applied to it. Assuming the magnetic field is in the z direction the resulting equation for one component of the current density is:

$$J_x \simeq \frac{j\omega\mu\sigma Ho(2a)}{\pi^2} \sum_{n_{odd}} \frac{4}{n^2} [\cos((n\pi/2a)x)] \left[\frac{\sinh((n\pi/2a)y)}{\cosh((n\pi/2a)h)}\right]. \quad (15)$$

The coordinates and variables used are shown in figure 1.

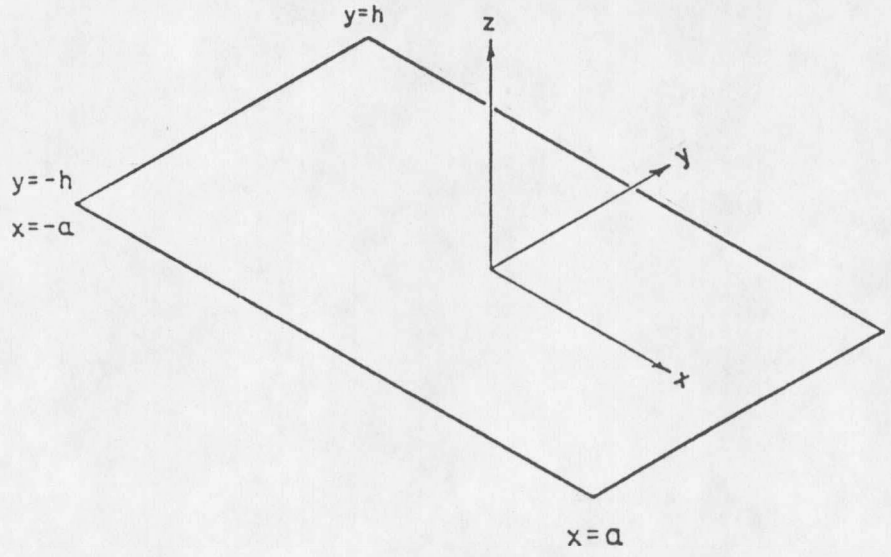

Figure 1. Coordinate system of rectangular conducting box.

The data from the Relaxation Method were compared with McLeod's analytical solution for the case of a square box. A box was chosen with the dimensions 5.25 mm. by 5.25 mm. with a conductivity of .71 mhos/cm., and a time-rate-of-change of the magnetic field of 5.3 Tesla/sec. This yielded a 43 by 43 grid with a spacing of .125 mm. in both directions. The driving parameters of the coil were chosen to be similar to ones now in clinical use. The comparison between the two yielded very similar results. For the analytic solution, the peak values of J_x, J_y, and the total magnitude were all .66722 microamps/cm^2, and for Relaxation Method they were 0.66618 microamps/cm^2. The maximum difference between the two methods was .01005 microamps/cm^2 (1.50% of the maximum value), with an average difference of $4.6 * 10^{-9}$ ($6.9*10^{-7}$%) for J_x and J_y, and $2.6*10^{-5}$ (.0039%) for the total magnitude. Finally, the correlation between the two methods was .9999968 for J_x and J_y, and 0.9999775 for the total magnitude. This clearly shows that both methods are converging to the same values. The difference can be attributed primarily to the numerical approximations made while calculating the spatial derivative of Hz.

Presentation of the Data for the Square Box Example

One of the problems encountered is how to present the data to researchers in different disciplines. A printout of an array of numbers is difficult to interpret. To further complicate matters the data are two-dimensional (J_x,J_y) over a two-dimensional area (the dimensions of the box). A combination of four methods were used to solve this problem.

The first method used to present the data is a "flow map" of the